Received: 2 February 2021 | Revised: 8 September 2021 | Accepted: 4 October 2021

DOI: 10.1002/hep.32184

ORIGINAL ARTICLE

Macrophage nuclear factor erythroid 2-related factor 2 deficiency promotes innate immune activation by tissue inhibitor of metalloproteinase 3–mediated RhoA/ROCK pathway in the ischemic liver

Jianhua Rao[1,2,3] | **Jiannan Qiu**[1,2] | **Ming Ni**[1,2] | **Hao Wang**[1,2] | **Peng Wang**[1,2] | **Lei Zhang**[1,2] | **Zeng Wang**[1,2] | **Mu Liu**[1,2] | **Feng Cheng**[1,2] | **Xuehao Wang**[1,2,3] | **Ling Lu**[1,2,3]

[1]Research Unit of Liver Transplantation and Transplant Immunology, Key Laboratory of Liver Transplantation, Chinese Academy of Medical Sciences, Hepatobiliary Center of The First Affiliated Hospital, Nanjing Medical University, Nanjing, China

[2]Jiangsu Key Lab of Cancer Biomarkers, Prevention and Treatment, Collaborative Innovation Center for Personalized Cancer Medicine, Nanjing Medical University, Nanjing, China

[3]State Key Laboratory of Reproductive Medicine, Nanjing, China

Correspondence
Ling Lu, Hepatobiliary Center of The First Affiliated Hospital, Nanjing Medical University, Nanjing 210029, China.
Email: lvling@njmu.edu.cn

or
Xuehao Wang, Hepatobiliary Center of The First Affiliated Hospital, Nanjing Medical University, Nanjing 210029, China.
Email: wangxh@njmu.edu.cn

or
Feng Cheng, Hepatobiliary Center of The First Affiliated Hospital, Nanjing Medical University, Nanjing 210029, China.
Email: docchengfeng@njmu.edu.cn

Abstract

Background and Aims: Nuclear factor erythroid 2-related factor 2 (Nrf2) is a master regulator of reactive oxygen species (ROS) and inflammation and has been implicated in both human and murine inflammatory disease models. We aimed to characterize the roles of macrophage-specific Nrf2 in liver ischemia/reperfusion injury (IRI).

Approach and Results: First, macrophage Nrf2 expression and liver injury in patients undergoing OLT or ischemia-related hepatectomy were analyzed. Subsequently, we created a myeloid-specific Nrf2-knockout ($Nrf2^{M\text{-}KO}$) strain to study the function and mechanism of macrophage Nrf2 in a murine liver IRI model. In human specimens, macrophage Nrf2 expression was significantly increased in liver tissues after transplantation or hepatectomy. Interestingly, lower Nrf2 expressions correlated with more severe liver injury postoperatively. In a mouse model, we found $Nrf2^{M\text{-}KO}$ mice showed worse hepatocellular damage than Nrf2-proficient controls based on serum biochemistry, pathology, ROS, and inflammation. In vitro, Nrf2 deficiency promoted innate immune activation and migration in macrophages on toll-like receptor (TLR) 4 stimulation. Microarray profiling showed Nrf2 deletion caused markedly lower transcriptional levels of tissue inhibitor of metalloproteinase 3 (Timp3). ChIP-seq, PCR, and luciferase reporter assay further demonstrated Nrf2 bound to

Abbreviations: ADAM, a disintegrin and metalloproteinase; BMM, bone marrow-derived macrophages; ChIP-seq, chromatin immunoprecipitation sequencing; GSH, glutathione; iNOS, inducible nitric-oxide synthase; IRI, ischemia/reperfusion injury; MCP, monocyte chemoattractant protein; MDA, malondialdehyde; MPO, myeloperoxidase; Nrf2, nuclear factor erythroid 2 -related factor 2; PHY, partial hepatectomy; POD1, first day postoperatively; RhoA, Ras homolog family member A; RNA-seq, RNA sequencing; ROCK1, Rho-associated coiled-coil containing protein kinase 1; ROS, reactive oxygen species; rTimp3, recombinant tissue inhibitor of metalloproteinase 3; sALT, serum alanine aminotransferase; sAST, serum aspartate aminotransferase; SCR-siRNA, scrambled control small interfering RNA; siRNA, small interfering RNA; Timp, tissue inhibitor of metalloproteinase; TLR, toll-like receptor; TUNEL, terminal deoxynucleotidyl transferase–mediated deoxyuridine triphosphate nick-end labeling; WB, western blot.

Jianhua Rao, Jiannan Qiu, and Ming Ni contributed equally to this work.

Funding information
The project was supported by the National Natural Science Foundation of China (81871259, 81971495, 82070675, 81530048, and 81570562), the Foundation of Jiangsu Collaborative Innovation Center of Biomedical Functional Materials, the Priority Academic Program Development of Jiangsu Higher Education Institutions, and the Six Talent Peaks Project in Jiangsu Province (2017-WSW-019) and the CAMS Innovation Fund for Medical Sciences (No. 2019-I2M-5-035).

the promoter region of Timp3. Moreover, a disintegrin and metalloproteinase (ADAM) 10/ROCK1 was specifically increased in Nrf2-deficient macrophages. Increasing Timp3 expression effectively inhibited ADAM10/ROCK1 expression and rescued the $Nrf2^{M\text{-}KO}$-mediated inflammatory response on TLR4 stimulation in vitro. Importantly, Timp3 overexpression, recombinant Timp3 protein, or ROCK1 knockdown rescued $Nrf2^{M\text{-}KO}$-related liver IRI by inhibiting macrophage activation.

Conclusions: In conclusion, macrophage Nrf2 mediates innate proinflammatory responses, attenuates liver IRI by binding to Timp3, and inhibits the RhoA/ROCK pathway, which provides a therapeutic target for clinical organ IRI.

INTRODUCTION

Hepatic ischemia/reperfusion injury (IRI) often occurs after liver transplantation, hemorrhagic shock, and hepatectomy and is an unresolved problem that confuses clinical doctors and patients.[1,2] The pathological process of liver IRI is characterized by the overproduction of reactive oxygen species (ROS), dysfunctional mitochondria, calcium overload, inflammatory cell recruitment, and the excess generation of proinflammatory cytokines.[1,3] In particular, inflammatory cells play vital roles in exacerbating hepatocellular apoptosis/necrosis during reperfusion.[4] High mobility group box 1, a danger-associated molecular pattern (DAMP) released by necrotic cells, directly activates the pattern recognition receptor system (including toll-like receptors [TLRs]), leading to local sterile inflammatory responses and further promoting hepatocellular apoptosis/necrosis.[5,6] Macrophages are the dominant immune cells in liver tissues and play a key role in activating innate immune responses to DAMPs. Thus, the regulation of macrophage-mediated innate immune response is key to attenuating liver IRI.

Nuclear factor erythroid 2-related factor 2 (Nrf2), a master regulator of antioxidative responses, is very crucial in maintaining cellular homeostasis. Nrf2 belongs to the NFE2 family of transcription factors and contains seven Neh domains that regulate Nrf2 activity by binding to DNA or proteins.[7] The Neh1 domain consists of a basic region-leucine zipper (bZIP) structure and is responsible for Nrf2 binding to DNA and dimerization with small Maf proteins, which are required for Nrf2 binding to antioxidant response elements (AREs) in the promoter regions of numerous cytoprotective genes and the initiation of transcription.[8] The Neh2 and Neh6 domains mediate the interaction with and regulation of Keap1 through the DLG and ETGE motifs.[9] This binding results in the ubiquitination and proteasomal degradation of Nrf2. The Neh3, Neh4, and Neh5 domains are transactivation domains. The Neh7 domain interacts with retinoid x receptor alpha, which represses Nrf2.[10] Under physiological conditions, Nrf2 is located in the cytoplasm, where it binds to Keap1 and undergoes sequestration, ubiquitination, and proteasomal degradation. However, under pathological conditions, Nrf2 is activated in two ways. (1) In canonical Nrf2 activation, specific cysteine residues on Keap1 are oxidized by oxidative stress or electrophiles, resulting in a conformational change in the adaptor protein and the inhibition of E3 ubiquitin ligase activity.[10,11] (2) In noncanonical Nrf2 activation, the Kir domain of p62 and Nrf2 share the same binding site with stretches of amino acids in Keap1, and p62 binding to Keap1 results in the release of Nrf2.[10,11] Activated Nrf2 translocases to the nucleus from the cytoplasm, leading to the transcription of multiple target genes, such as Gpx2, Nqo1, and Hmox1.[12]

Nrf2-driven regulation of antioxidant and anti-inflammatory effects is important for cytoprotection and defense. Previous studies have demonstrated that Nrf2 disruption increases the severity of ischemia-related injury in the kidney, brain, and heart.[13,14] In contrast, activation of Nrf2 has been reported to protect against cerebral, retinal, cardiac, and intestinal IR-induced tissue damage.[15-17] An increasing number of studies have also illustrated the functions of Nrf2 during liver IRI,[18-21] but Nrf2 may affect liver IRI through both parenchymal (hepatocytes) and nonparenchymal cells (macrophages, NK cells, and so on) because of its different roles in various cell types and cellular activities. The involvement of macrophage Nrf2 in hepatic IRI has not been well investigated to date, partly because of the lack of cell-specific tools for in vivo analysis.

It is reported that transient receptor potential vanilloid 1–evoked Ca^{2+} influx promoted the phosphorylation of calcium/calmodulin-dependent protein kinase II and facilitated the nuclear localization of Nrf2, which ultimately resulted in the inhibition of macrophage M1 polarization in the osteoarthritis.[22] Auranofin-mediated Nrf2 induction attenuated IL-1β expression in lipopolysaccharide (LPS)-stressed alveolar macrophages, which further

suppressed macrophage-mediated inflammation.[23] In addition, the relation between Nrf2 and RhoA/ROCK1 has been reported. For example, the Nrf2/Keap1 pathway may affect cell motility by dysregulating the RhoA/ROCK1 signaling in non-small-cell lung cancer cells.[24] Moreover, Nrf2 could promote breast cancer cell proliferation and metastasis by increasing RhoA/ROCK pathway signal transduction.[25] However, there is no report exploring the relation between Nrf2 and tissue inhibitor of metalloproteinase (Timp) 3.

Herein, we hypothesized that macrophage Nrf2 is critical for innate immune activation and liver injury during liver IRI. First, macrophage Nrf2 expression and liver function in patients undergoing OLT or ischemia-related hepatectomy were assessed. Second, we created a myeloid-specific Nrf2-knockout ($Nrf2^{M\text{-}KO}$) strain to study the function and mechanism of macrophage Nrf2 in liver IRI. Third, the functional roles and molecular mechanisms of macrophage Nrf2 were deeply analyzed in vivo and in vitro.

PATIENTS AND METHODS

Patients and clinical samples

The study was approved by the Research Ethics Committee of the First Affiliated Hospital of Nanjing Medical University in Nanjing, China (Institutional Review Board approval number 2018-SRFA-197). Informed consent in writing was obtained from each patient and the study protocol conformed to the ethical guidelines of the 1975 Declaration of Helsinki as reflected in a priori approval by the appropriate institutional review committee. Biopsy specimens were obtained from 30 patients (Table S1) with end-stage liver disease undergoing OLT at Hepatobiliary Center of the First Affiliated Hospital of Nanjing Medical University between January 2019 and December 2019. Pre-OLT hepatic biopsies were harvested from the left lobe during back-table preparation (before implantation), and post-OLT hepatic biopsies were harvested at 2-3 h after portal reperfusion (before abdominal closure). All organ donations recorded in the electronic database were contributed voluntarily without donors from executed prisoners or other institutionalized persons. Nonfatty donor organs, which were procured according to standardized techniques, were perfused with and stored in cold University of Wisconsin (UW) solution. The ischemia time was defined as the time between the perfusion of the donor liver with UW solution and its removal from cold storage. Additionally, biopsy specimens were obtained from 30 patients (Table S2) with benign liver disease undergoing partial hepatectomy (PHY) with the Pringle maneuver (January 2019-December 2019, Hepatobiliary Center, the First Affiliated Hospital of Nanjing Medical University). Prehepatectomy hepatic biopsies were harvested after laparotomy (before hepatic portal occlusion), and posthepatectomy hepatic biopsies were obtained after reperfusion (before abdominal closure). The ischemia time was between 15 and 30 min. Serum alanine aminotransferase (sALT) was measured on the first day postoperatively (POD1) to assess the degree of hepatocellular injury. Informed consent was obtained from all participants.

Hepatic IRI model and treatments

Nrf2-LoxP mice ($Nrf2^{FL/FL}$) were bred with myeloid-specific Cre mice (Lyz2-Cre) to create myeloid-specific Nrf2-KO mice ($Nrf2^{M\text{-}KO}$). Male $Nrf2^{FL/FL}$ and $Nrf2^{M\text{-}KO}$ mice (6-8-week-old) on a C57BL/6 background (Nanjing Biomedical Research Institute of Nanjing University) were used in the experiments. The procedure to establish the mouse hepatic IRI model was the same as that described in previous studies.[2,7,8] Briefly, the arterial/portal vessels to the cephalad lobes were clamped for 90 min. However, there was no vascular occlusion in sham-controlled mice. The severity of the pathological injury was graded blindly using Suzuki's criteria on a scale from 0 to 4. In the treatment groups, each mouse was injected through the portal vein with 5×10^6 bone marrow-derived macrophages (BMMs) transfected with Ad-Timp3/Ad-β-gal (2.5×10^9 plaque-forming units) or untreated BMMs 24 h before the onset of warm ischemia. After the adoptive transfer of Ad-β-gal-transfected BMMs, X-Gal staining in the ischemic liver lobes after 6 h of reperfusion was 40-50% compared with that of the control livers.[8,26] Additionally, 4 h before the establishment of the hepatic IR model, some mice were injected through the tail vein with ROCK1-small interfering RNA (siRNA) or scrambled control siRNA (SCR-siRNA) (2 mg/kg) mixed with mannose-conjugated polymers (Polyplus-transfection) at a ratio based on the manufacturer's instructions.[27] Recombinant Timp3 (rTimp3) (100 ng/kg body weight, EMD Bioscience) was administered to mice 1 h before establishing the IRI model.[28]

Cesium source was used to irradiate male $Nrf2^{FL/FL}$ mice (5-week-old) twice with a dose of 550 rad (5.5 Gy) 4 h before transplantation. Bone marrow was isolated from femurs of $Nrf2^{FL/FL}$ or $Nrf2^{M\text{-}KO}$ mice by flushing with sterile Opti-MEM (Thermo Fisher Scientific). The 1×10^7 BMMs were injected into each recipient mouse through retro-orbital injection. Bone marrow transplantations were performed to generate the chimeric mice as follows: $Nrf2^{FL/FL}$ mice reconstituted with $Nrf2^{FL/FL}$ BMMs (FL/FL→FL/FL) and $Nrf2^{FL/FL}$ mice reconstituted with $Nrf2^{M\text{-}KO}$ BMMs (M-KO→FL/FL). The chimeras would be subjected to the liver IR injury model after 4 weeks from bone marrow transplantation. The neutrophil depletion was performed with an intraperitoneal injection of 500 μg anti-Ly6G antibody (1A8, BioXCell) 24 and 2 h before establishing IRI model and the control mice were injected with anti-IgG.

Statistical analysis

All data in this study are presented as the mean ± SD. We used SPSS software ver. 20.0 and GraphPad Prism 8.0 to analyze the data and calculate the *p* values. Statistical differences between multiple groups were evaluated using Student's *t* tests or ANOVA. All experiments were repeated at least three times, and the differences were deemed statistically significant when the *p* value < 0.05.

For further details regarding the methods and materials, please refer to the Supporting Material.

RESULTS

Nrf2 expression in macrophages is increased and negatively correlates with IR stress-induced liver injury in patients

To explore the role of macrophage Nrf2 in the pathogenesis of hepatic IRI, we first examined Nrf2 expression in macrophages of liver specimens from 30 patients undergoing OLT. Nrf2 expression was examined in macrophages extracted from fresh liver tissues and further purified with CD68 magnetic beads. Figure 1A showed the expression of Nrf2 significantly increased in liver macrophages after reperfusion. Interestingly, the postoperative Nrf2 levels correlated negatively with sALT values at POD1 (Figure 1B: R^2 = 0.4468, p < 0.0001). In addition, we divided the patients into low-Nrf2 and high-Nrf2 groups using the median ratio of Nrf2/GAPDH as the threshold (Figure 1C: threshold = 0.922). Compared with the low Nrf2 group, patients with higher Nrf2 levels exhibited lower sALT levels at POD1 (Figure 1D). Similarly, hematoxylin and eosin (H&E) staining and terminal deoxynucleotidyl transferase–mediated deoxyuridine triphosphate nick-end labeling (TUNEL) staining displayed that the low Nrf2 group featured worsened sinusoidal congestion, edema, vacuolization, and apoptosis (Figure 1E).

Then, we examined Nrf2 expression in liver macrophages from 30 patients undergoing PHY. Figure 1F exhibited the higher Nrf2 expression of macrophages from posthepatectomy in comparison to prehepatectomy. The postoperative Nrf2 levels correlated negatively with sALT values at POD1 (Figure 1G: R^2 = 0.6747, p < 0.0001). These patients were also divided into low-Nrf2 and high-Nrf2 groups using the median of postoperative Nrf2/GAPDH ratio as the threshold (Figure 1H: threshold = 0.627). Unlike the low Nrf2 group, patients who were characterized by higher Nrf2 levels exhibited lower sALT levels at POD1 (Figure 1I). The H&E and TUNEL staining results showed that the low Nrf2 group held more severe sinusoidal congestion, edema, vacuolization, and apoptosis (Figure 1J).

Myeloid-specific Nrf2 deficiency exacerbates IR-induced hepatocellular damage

To better clarify the role of macrophage Nrf2 in regulating hepatocellular damage, ROS production, and inflammation during hepatic IR, we used the *Cre-LoxP* system to create myeloid-specific Nrf2-KO ($Nrf2^{M\text{-}KO}$) mice. The overall expression levels of Nrf2 in livers or hepatocytes from $Nrf2^{FL/FL}$ and $Nrf2^{M\text{-}KO}$ mice showed no significant differences. Hepatic nonparenchymal cells and BMMs isolated from $Nrf2^{M\text{-}KO}$ mice showed significantly lower levels of Nrf2 than those isolated from $Nrf2^{FL/FL}$ mice (Figure 2A). After 90 min of warm ischemia followed by 6 h of reperfusion, compared with $Nrf2^{FL/FL}$ mice, $Nrf2^{M\text{-}KO}$ mice exhibited severe edema, sinusoidal congestion, vacuolization, and extensive hepatocellular necrosis, which correlated with Suzuki's histological grading of hepatic IR injury (Figure 2B,C). Increased sALT and serum aspartate aminotransferase (sAST) levels were detected in $Nrf2^{M\text{-}KO}$ mice, which also indicated worsened hepatocellular injury (Figure 2D). $Nrf2^{M\text{-}KO}$ mice displayed elevated myeloperoxidase (MPO) levels, reflecting liver neutrophil activity (U/g) (Figure 2E). Moreover, myeloid-specific Nrf2 deficiency significantly worsened IR-induced ROS and malondialdehyde (MDA) production and reduced glutathione (GSH) activity in ischemic livers (Figure 2F). TUNEL staining revealed an increased number of TUNEL-positive cells in ischemic livers from $Nrf2^{M\text{-}KO}$ mice (Figure 2G,H). Western blot (WB) analysis also showed that the antiapoptotic proteins Bcl-2 and Bcl-xl were down-regulated in ischemic livers from $Nrf2^{M\text{-}KO}$ mice (Figure 2I). To exclude the effect of Nrf2 in polymorphonuclear neutrophils during liver IR injury, we first established the chimeric mice through irradiation and BMMs transplantation. The corroborating results showed that Nrf2-deficiency macrophage promoted IR-induced liver injury, as evidence by the higher levels of sALT and sAST and more severe histological injury in $Nrf2^{FL/FL}$ mice reconstituted with $Nrf2^{M\text{-}KO}$ BMMs (Figure S1A-C). Then, we used the anti-Ly6G antibody to eliminate the neutrophils (Figure S1D,E). As shown in Figure S1F-H, $Nrf2^{M\text{-}KO}$ mice suffered more drastic IR injury than $Nrf2^{FL/FL}$ mice, regardless of anti-Ly6G antibody treatment. The results revealed that the elimination of neutrophils failed to offset the huge difference in IR-induced liver injury between $Nrf2^{FL/FL}$ and $Nrf2^{M\text{-}KO}$ mice.

Myeloid-specific Nrf2 deficiency increases macrophage/neutrophil infiltration and proinflammatory mediators in IR stress-induced livers

Given that activation of the innate immune response plays an essential role in exacerbating hepatic IRI, we evaluated the accumulation of hepatic inflammatory

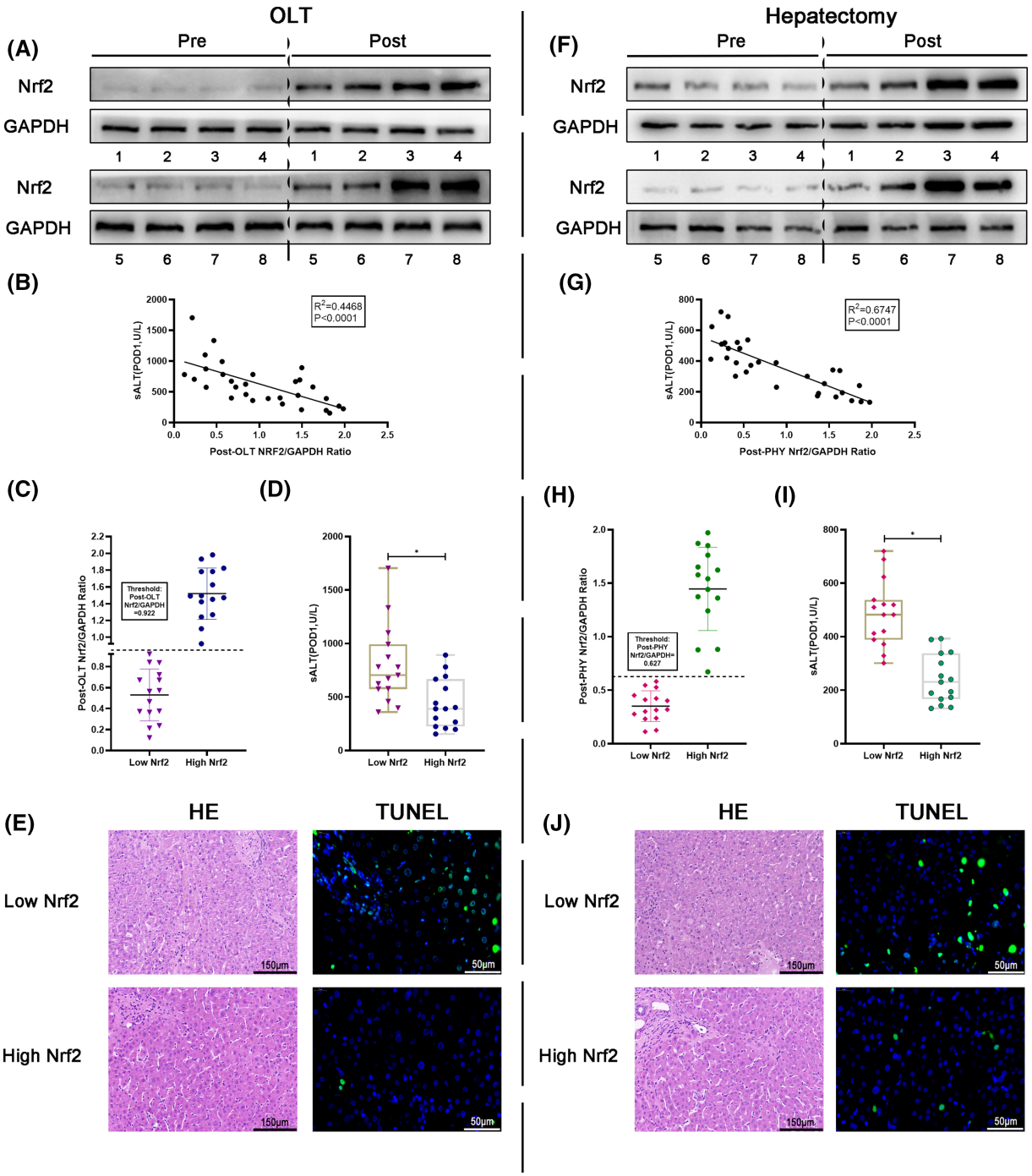

FIGURE 1 Nrf2 expression in macrophages is increased and negatively correlates with IR stress-induced liver injury in patients. Liver macrophages were isolated from 30 patients undergoing OLT (A-E) or 30 patients undergoing PHY (F-J). (A) WB-assisted pre/post-OLT Nrf2 expression profiles in macrophages (representative eight cases). (B) The ratio of post-OLT Nrf2/GAPDH correlated negatively with sALT at POD1. (C) Thirty human OLTs were divided into low (n = 15) and high (n = 15) ratio group of post-OLT Nrf2/GAPDH using the median of postoperative Nrf2/GAPDH ratio as the threshold (threshold = 0.922). (D) sALT values in both Low Nrf2 and High Nrf2 groups in OLT recipients at POD1; *p < 0.05 by Student t test. (E) HE staining and TUNEL staining in OLT biopsies. (F) WB-assisted prehepatectomy and posthepatectomy Nrf2 expression profiles in macrophages (representative eight cases). (G) The ratio of posthepatectomy Nrf2/GAPDH correlated negatively with sALT at POD1. (H) Thirty human hepatectomy were divided into low (n = 15) and high (n = 15) ratio group of post-OLT Nrf2/GAPDH using the median of postoperative Nrf2/GAPDH ratio as the threshold (threshold = 0.627). (I) sALT values in both Low Nrf2 and High Nrf2 groups in hepatectomy patients at POD1; *p < 0.05 by Student t test. (J) HE staining and TUNEL staining in posthepatectomy biopsies

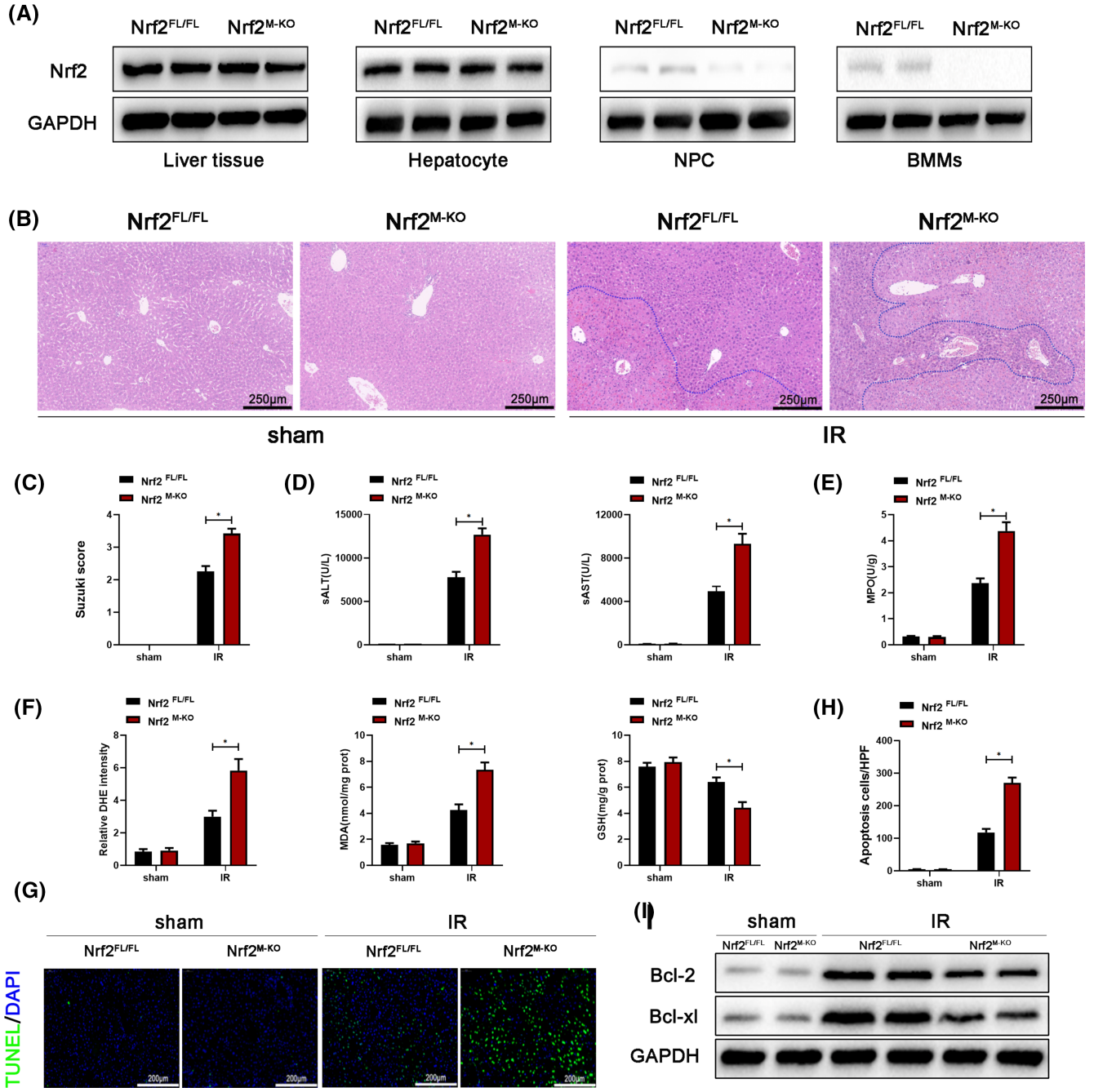

FIGURE 2 Myeloid-specific Nrf2 deficiency aggravates IR-induced hepatocellular damage. The IR model mice were subjected to 90 min of partial liver warm ischemia, followed by 6 h of reperfusion. (A) WB-assisted Nrf2 expression profiles in liver tissues, hepatocytes, macrophages, nonparenchymal cells (NPCs), and BMMs from $Nrf2^{FL/FL}$ and $Nrf2^{M\text{-}KO}$ mice. (B) Representative HE staining of ischemic liver tissues, Scale is 250 μm. (C) Liver damage was evaluated by Suzuki's histological score. (D) sALT and sAST levels were measured from sham and IR groups. (F) MPO activities of liver tissues. (F) Quantitation of ROS-sensing dye DHE staining, MDA, and GSH activities were assessed in ischemic liver tissues. (G,H) TUNEL staining of liver tissues; positive cell percentage was evaluated. (I) WB-assisted Bcl-2 and Bcl-xl expression profiles in liver tissues. $n = 6$, $^*p < 0.05$ by Student t test

cells by F4/80 and CD11b (macrophage markers) and Ly6G (a neutrophil marker) staining after IRI. Compared with $Nrf2^{FL/FL}$ mice, myeloid-specific Nrf2 deficiency markedly increased macrophage and neutrophil infiltration in IR stress-induced livers (Figure 3A-C). The flow cytometry analysis furthermore confirmed that the population of neutrophils and macrophages was markedly increased in the IR-stressed livers of $Nrf2^{M\text{-}KO}$ mice compared with $Nrf2^{FL/FL}$ mice (Figure 3D). Unlike $Nrf2^{FL/FL}$ mice, $Nrf2^{M\text{-}KO}$ mice exhibited increased levels of TNF-α, IL-6, monocyte chemoattractant protein (MCP)-1, and inducible nitric-oxide synthase (iNOS) and reduced levels of IL-10 in IR stress-induced livers (Figure 3E). Consistent with

the mRNA data, increased levels of serum TNF-α, IL-6, and MCP-1 and decreased levels of IL-10 were detected in Nrf2$^{M\text{-}KO}$ mice after IRI (Figure 3F).

Myeloid-specific Nrf2 deficiency exacerbates sterile inflammation

Expression of Nrf2 in BMMs isolated from Nrf2$^{FL/FL}$ mice was significantly elevated in response to LPS stimulation (100 ng/mL, 6 h) (Figure 4A). TLR4-mediated innate immunity activation plays an essential role in triggering hepatic inflammation and activating NF-κB and inflammatory mediators, leading to local sterile inflammation. Increased mRNA levels of TNF-α, IL-6, MCP-1, and iNOS and reduced levels of IL-10 in BMMs isolated from Nrf2$^{M\text{-}KO}$ mice in response to LPS stimulation (100 ng/mL, 3 h) were measured by qRT-PCR (Figure 4B). Moreover, Nrf2 deficiency promoted the production of TNF-α, IL-6, and MCP-1 but inhibited the production of IL-10 in the culture media of BMMs treated with LPS for 24 h (Figure 4C). Because of the release of multiple chemokines, we also examined the effect of Nrf2 on macrophage migration in vitro. First, we isolated BMMs from Nrf2$^{FL/FL}$ and Nrf2$^{M\text{-}KO}$ mice, cultured them for 7 days, and then stimulated the cells with or without LPS for 24 h. The supernatant was collected and used as the conditioned medium. Transwell assays showed that the migratory ability of BMMs was markedly enhanced by the indicated conditioned medium. More importantly, Nrf2 deficiency promoted the migration of BMMs in an inflammatory environment (Figure 4D). Furthermore, Nrf2 deficiency up-regulated PTEN and TLR4/NF-κB expression but down-regulated Akt phosphorylation in LPS-stimulated BMMs (Figure 4E).

Nrf2 directly regulates Timp3 to mediate the RhoA/ROCK pathway

To explore the underlying mechanism by which macrophage Nrf2 regulates the acute inflammatory response, RNA sequencing (RNA-seq) was performed to identify genes that were differentially expressed in LPS-stimulated BMMs from Nrf2$^{FL/FL}$ and Nrf2$^{M\text{-}KO}$ mice. The RNA-seq results indicated that Timp3 was markedly down-regulated in Nrf2-deficient BMMs stimulated with LPS (Figure 5A). Moreover, the NF-κB pathway was likely involved in the regulation of Nrf2 in BMMs based on the results of the Kyoto Encyclopedia of Genes and Genomes analysis (Figure 5B). Then, we performed Nrf2 ChIP coupled to massively parallel sequencing (ChIP-Seq). Nrf2 ChIP-seq peaks were identified within the Timp3 gene. One peak was located in the promoter region, and the others were located within the intron or exon (Figure 5C). ChIP-PCR was performed using an anti-Nrf2 antibody in LPS-treated BMMs to verify that the ChIP-seq peak was located in the Timp3 promoter region. After ChIP with the Nrf2 antibody, primers were designed to detect the Nrf2/TCF DNA-binding site in the Timp3 promoter by PCR, which verified that Nrf2 was located on the promoter of Timp3. Therefore, Timp3 is a target gene regulated by Nrf2 (Figure 5D). Then, a luciferase reporter assay was performed to verify whether Nrf2 is bound to the Timp3 promoter to regulate transcription. The relative luciferase activity was strongest when 293T cells were transfected with plasmid-Nrf2 and plasmid-Timp3-Promoter (Figure 5E). In short, Timp3 is a target gene that is positively regulated by Nrf2. Consistent with the RNA-seq results, reduced mRNA levels of timp3 and increased mRNA levels of ROCK1 were detected in Nrf2-deficient BMMs stimulated with LPS (Figure 5F). Moreover, the protein level of Timp3 was markedly decreased, which contributed to the increased protein levels of ADAM10 and ROCK1, which was consistent with activation of the NF-κB signaling pathway (Figure 4E) in LPS-stimulated Nrf2-deficient BMMs compared with that of the controls (Figure 5G). Then, we isolated the hepatic macrophages from Nrf2$^{FL/FL}$ and Nrf2$^{M\text{-}KO}$ mice after establishing the sham or IR model. Consistent with in vitro results, Nrf2 deficiency also reduced the Timp3 expression and subsequently enhanced ADAM10/ROCK1/TLR4 pathway in macrophages from ischemic livers (Figure 5H).

Adoptive transfer of Ad-Timp3 BMMs or rTimp3 administration prevents IR-induced hepatocellular damage in Nrf2$^{M\text{-}KO}$ mice

BMMs were isolated from Nrf2$^{M\text{-}KO}$ mice and cultured for 7 days. After transfection with Ad-Timp3 or Ad-β-gal, these BMMs were incubated with LPS for 6 h. WB showed that the expression of ADAM10, ROCK1, and TLR4/NF-κB was inhibited when Timp3 was overexpressed in Nrf2-deficient BMMs (Figure 6A). Moreover, immunofluorescence staining showed that ROCK1 expression was inhibited in BMMs transfected with Ad-Timp3 (Figure 6B). Consistent with the previous data, the mRNA levels of TNF-α, IL-6, iNOS, and MCP-1 were reduced, but the mRNA levels of IL-10 were increased in Timp3-transfected BMMs isolated from Nrf2$^{M\text{-}KO}$ mice compared with those of the control group and Ad-β-gal group (Figure 6C). The migratory ability of Nrf2-deficient BMMs was inhibited when Timp3 was overexpressed (Figure 6D). These data demonstrate that Timp3 is critical for the Nrf2-regulated ROCK pathway in macrophages.

Nrf2$^{M\text{-}KO}$ mice were subjected to IRI after the infusion of Ad-Timp3 Nrf2$^{M\text{-}KO}$ BMMs, Ad-β-gal Nrf2$^{M\text{-}KO}$ BMMs, or untreated Nrf2$^{M\text{-}KO}$ BMMs as controls (Figure 6E). In this model, the IR stress-induced livers from Nrf2$^{M\text{-}KO}$ mice that were preconditioned with

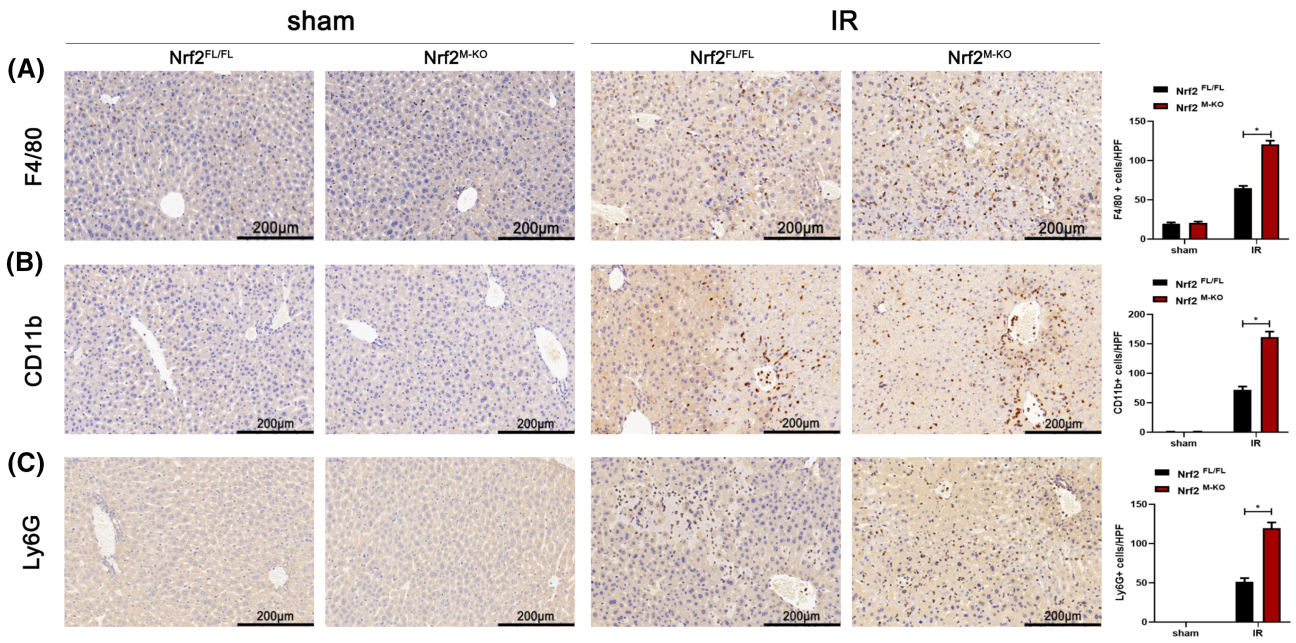
sham
IR
Nrf2FL/FL
Nrf2M-KO
(A)
F4/80
(B)
CD11b
(C)
Ly6G
200μm
Nrf2 FL/FL
Nrf2 M-KO
F4/80 + cells/HPF
CD11b+ cells/HPF
Ly6G+ cells/HPF
sham
IR

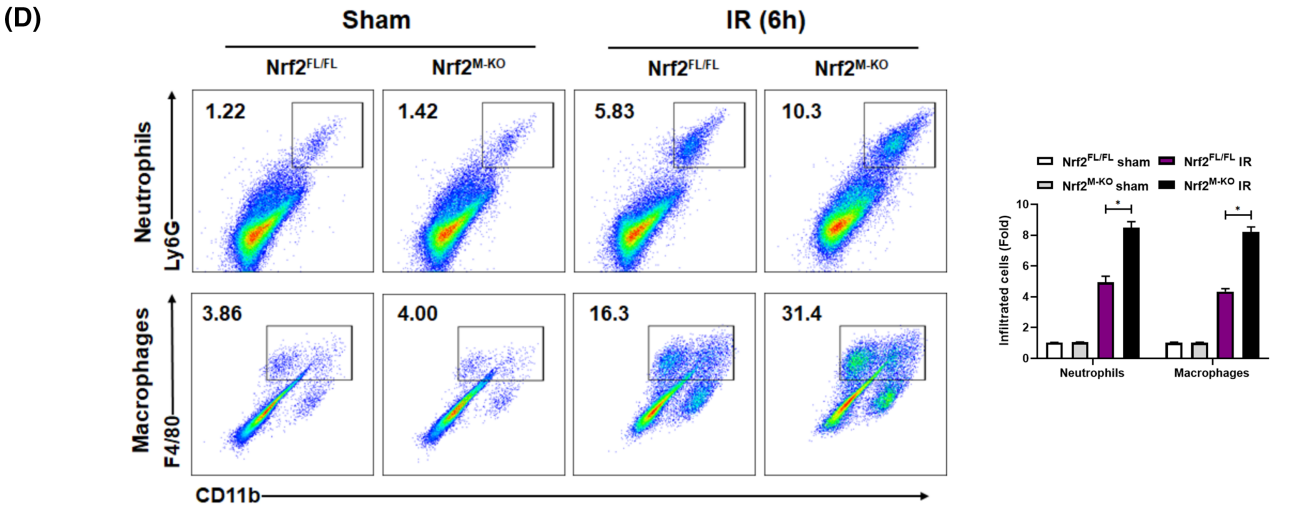
(D)
Sham
IR (6h)
Nrf2FL/FL
Nrf2M-KO
Neutrophils
Ly6G
Macrophages
F4/80
CD11b
1.22
1.42
5.83
10.3
3.86
4.00
16.3
31.4
Nrf2FL/FL sham
Nrf2FL/FL IR
Nrf2M-KO sham
Nrf2M-KO IR
Infiltrated cells (Fold)
Neutrophils
Macrophages

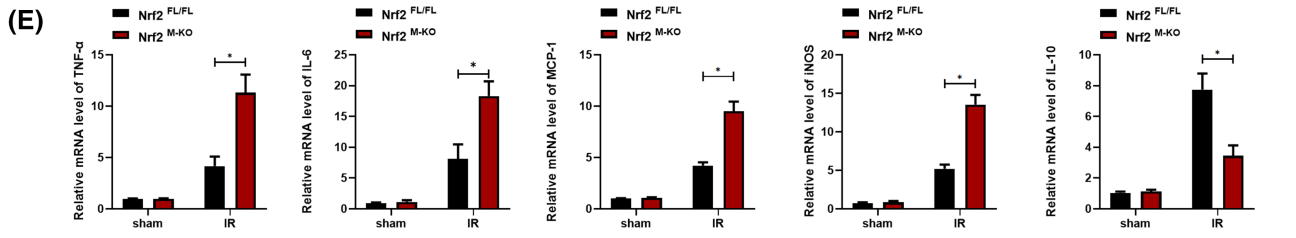
(E)
Nrf2 FL/FL
Nrf2 M-KO
Relative mRNA level of TNF-α
Relative mRNA level of IL-6
Relative mRNA level of MCP-1
Relative mRNA level of iNOS
Relative mRNA level of IL-10
sham
IR

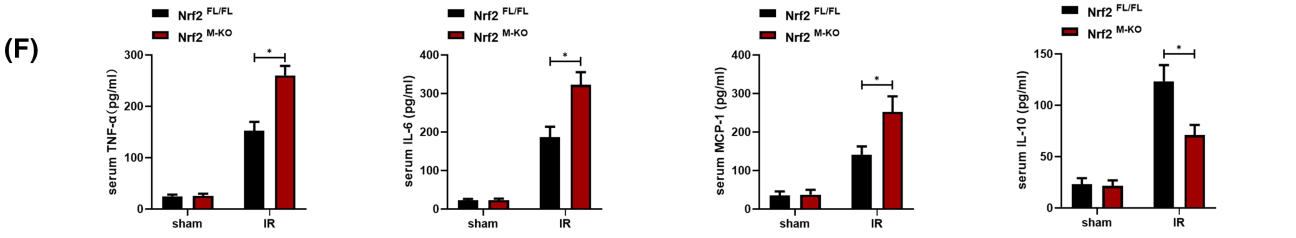
(F)
Nrf2 FL/FL
Nrf2 M-KO
serum TNF-α (pg/ml)
serum IL-6 (pg/ml)
serum MCP-1 (pg/ml)
serum IL-10 (pg/ml)
sham
IR

FIGURE 3 Myeloid-specific Nrf2 deficiency promotes inflammatory responses in IR-stressed livers. The IR model mice were subjected to 90 min of partial liver warm ischemia, followed by 6 h of reperfusion. (A,B) Macrophage infiltration were analyzed by immunohistological staining with antibodies against F4/80 or CD11b; F4/80+ or CD11b+ cells were quantitated by counting numbers of positive cells/area. Scale is 200 μm. (C) Neutrophil infiltration was analyzed by immunohistological staining with antibodies against Ly6G; Ly6G+ cells were quantitated by counting numbers of positive cells/area. Scale is 200 μm. (D) Flow cytometry analysis was conducted to examine the accumulation of neutrophils and macrophages in livers from mice subjected to 6 h postreperfusion. (E) Detection of TNF-α, IL-6, MCP-1, iNOS and IL-10 by qRT-PCR in ischemic livers. (F) Detection of TNF-α, IL-6, MCP-1, and IL-10 by ELISA in serum. $n = 6$, $^*p < 0.05$ by Student t test

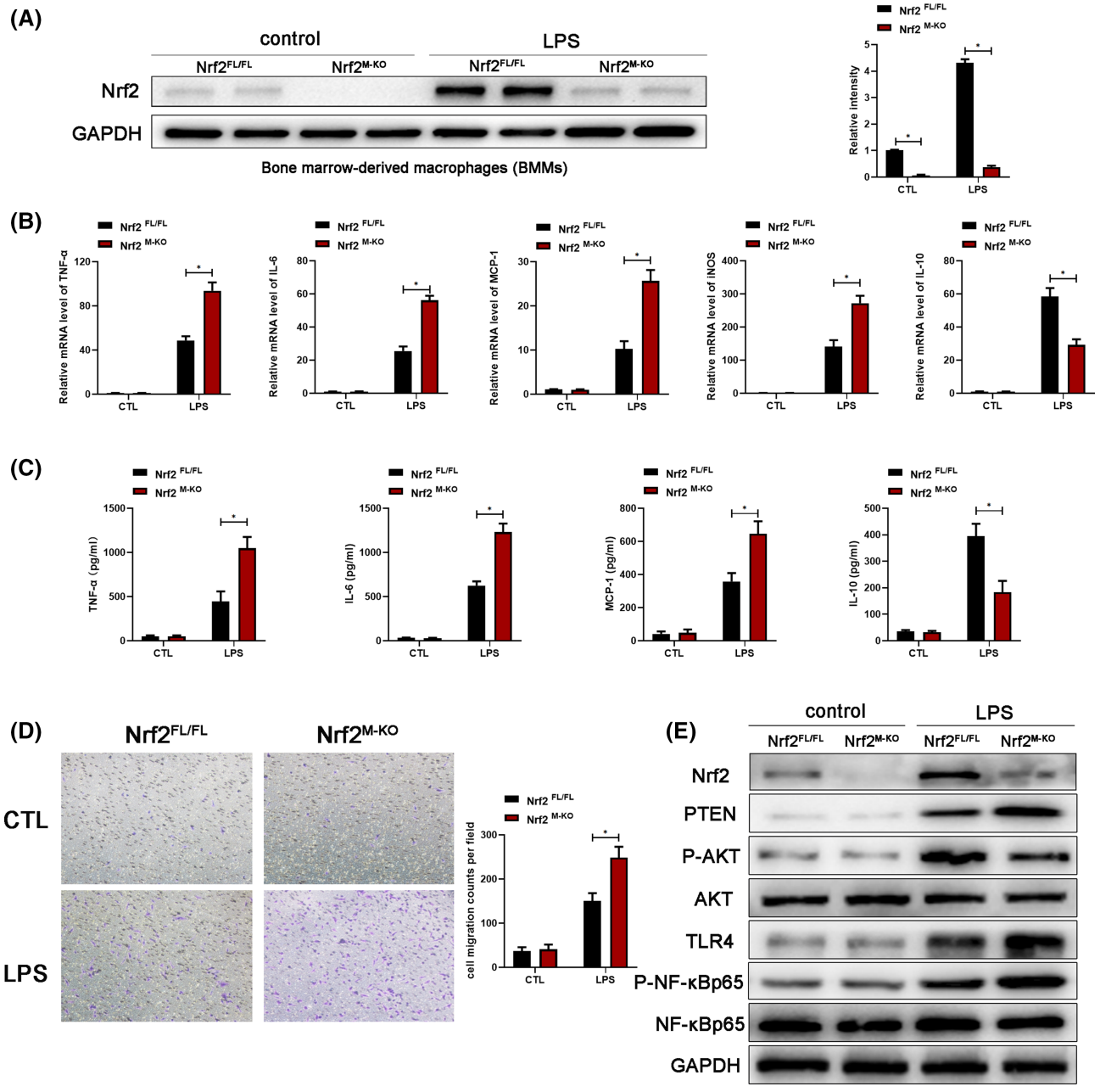

FIGURE 4 Myeloid-specific Nrf2 deficiency aggravates innate inflammatory responses. BMMs were isolated from $Nrf2^{FL/FL}$ and $Nrf2^{M\text{-}KO}$ mice. (A) WB-assisted Nrf2 expression profiles in BMMs cultured with LPS (100 ng/mL, 6 h). (B) Detection of TNF-α, IL-6, MCP-1, iNOS, and IL-10 by qRT-PCR in BMMs cultured with LPS (100 ng/mL, 3 h). (C) Detection of TNF-α, IL-6, MCP-1, and IL-10 by ELISA in supernatant. (D) Transwell assay analyzed the migratory ability of BMMs with LPS for 24 h. (E) Nrf2, PTEN, P-AKT, AKT, TLR4, P-NF-κBp65, and NF-κBp65 protein expression levels measured by WB. Representative of three experiments. BMMs were treated with LPS (100 ng/mL) stimulation for 6 h; untreated BMMs were used as controls. $n = 4\text{-}6$, $^*p < 0.05$ by Student t test

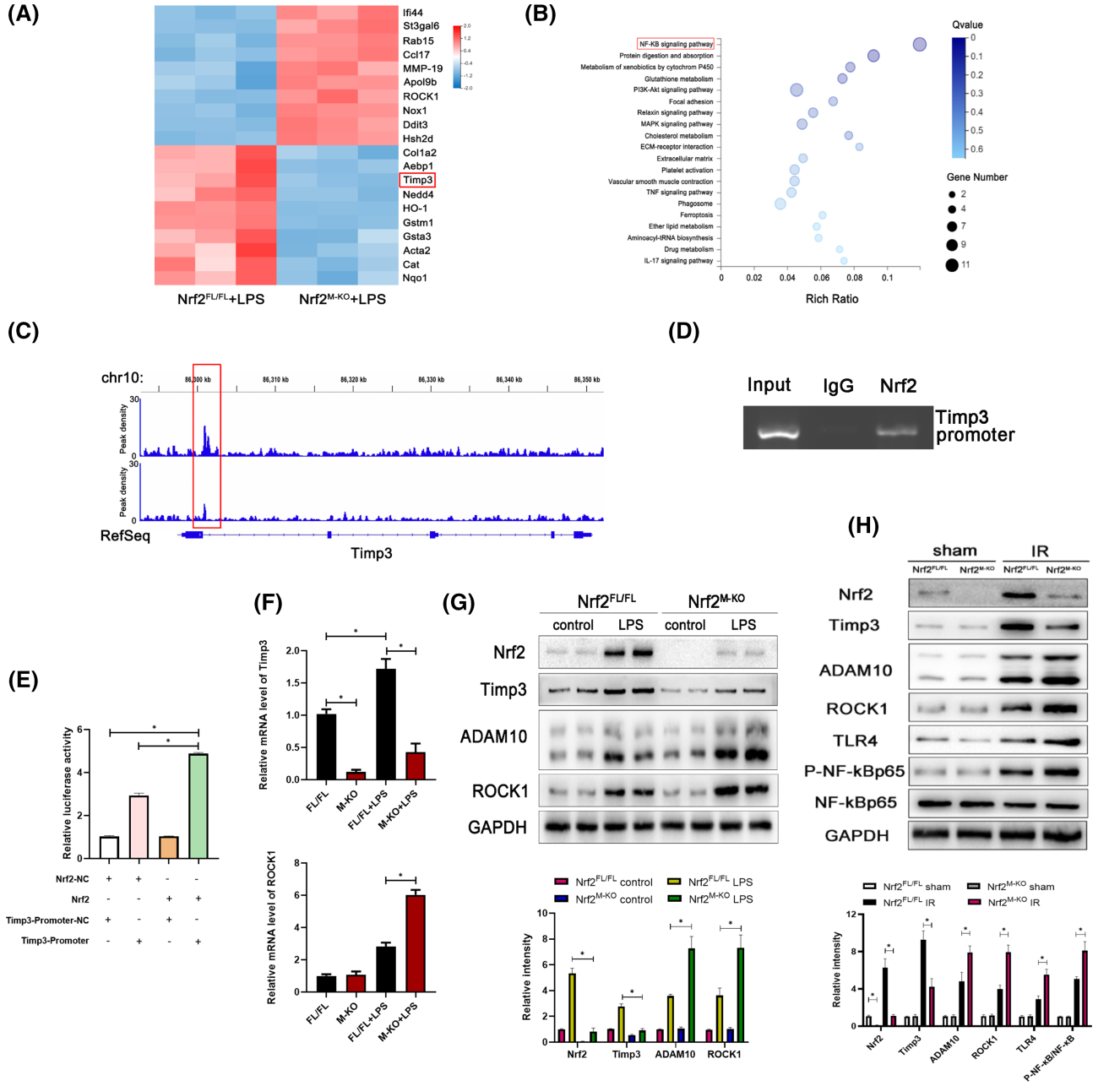

FIGURE 5 Nrf2 directly regulated Timp3 to orchestrate RhoA/ROCK pathway. (A) The heatmap shows differently expressed genes in LPS-stimulated BMMs from $Nrf2^{FL/FL}$ and $Nrf2^{M\text{-}KO}$ mice. (B) Kyoto Encyclopedia of Genes and Genomes pathway enrichment analysis of the identified differentially expressed genes. (C) Nrf2 ChIP-seq peaks were identified within the Timp3 gene. (D) ChIP-PCR analysis of Nrf2 binding to the Timp3 promoter. (E) Luciferase reporter assay of 293T cells transfected with plasmid-Nrf2 or plasmid-NC and plasmid-Timp3-Promoter or plasmid-Timp3-Promoter-NC. (F) qPCR analysis for the relative mRNA level of Timp3 and ROCK1 in different groups. (G) WB analysis of the protein levels of Nrf2, Timp3, ADAM10, ROCK1, and GAPDH in different groups. (H) WB analysis of the protein levels of Nrf2, Timp3, ADAM10, ROCK1, TLR4, P-NF-κB, NF-κB, and GAPDH in macrophage from different groups. $n = 4\text{-}6$, $^*p < 0.05$ by Student *t* test

Ad-Timp3 $Nrf2^{M\text{-}KO}$ BMMs exhibited reduced levels of sALT and sAST and inhibited MPO activity (Figure 6F). Moreover, the infusion of Ad-Timp3 $Nrf2^{M\text{-}KO}$ BMMs alleviated IR-induced ROS and MDA production and increased GSH activity in ischemic livers (Figure 6G). Figure 6H,I showed that the IR stress-induced livers from $Nrf2^{M\text{-}KO}$ mice that were preconditioned with Ad-β-gal or untreated $Nrf2^{M\text{-}KO}$ BMMs exhibited worsened edema, sinusoidal congestion, and cytoplasmic vacuolization, and extensive hepatocellular apoptosis and necrosis. The infiltration of inflammatory cells was significantly increased in the IR stress-induced livers from $Nrf2^{M\text{-}KO}$ mice that were preconditioned with Ad-β-gal or untreated $Nrf2^{M\text{-}KO}$ BMMs (Figure 6J-M). $Nrf2^{M\text{-}KO}$ mice that were preconditioned with Ad-Timp3 BMMs exhibited reduced mRNA levels of TNF-α and iNOS

and increased IL-10 level in IR stress-induced livers (Figure 6N).

Based on the clinical importance of therapeutics, we treated Nrf2$^{M\text{-}KO}$ mice with rTimp3 or PBS as a control before establishing the hepatic IRI model (Figure 7A). rTimp3 treatment significantly alleviated IR-induced hepatocellular damage (Figure 7B-D), macrophage/neutrophil infiltration, and proinflammatory mediators in IR stress-induced livers (Figure 7E-H); reduced IR-induced ROS and MDA production; and increased GSH activity in ischemic livers from Nrf2$^{M\text{-}KO}$ mice (Figure 7I).

Inhibiting the ROCK pathway rescues myeloid-specific Nrf2 deficiency-related inflammation and injury in ischemic livers

To confirm whether the induction of the hepatic innate immune response and IR-induced inflammatory injury depends on the activation of the ROCK pathway in the livers of Nrf2$^{M\text{-}KO}$ mice, mannose-conjugated polymers were used to deliver ROCK1-siRNA or SCR-siRNA in vivo (Figure 8A). Mannose-mediated siRNA expresses a mannose-specific membrane receptor, which can be specifically delivered to macrophages/KCs, as previously reported.[27,29] After 90 min of warm ischemia followed by 6 h of reperfusion, a reduction in IR-induced liver injury was detected in Nrf2$^{M\text{-}KO}$ mice after treatment with mannose-mediated ROCK1-siRNA, as evidenced by reduced sALT and sAST levels (Figure 8B); Suzuki scores (Figure 8D), which consisted with the well-preserved hepatic architecture, sinusoidal congestion, edema, vacuolization, necrosis (Figure 8C); and MPO levels (Figure 8E) compared with those of SCR-siRNA–treated Nrf2$^{M\text{-}KO}$ mice. The TUNEL staining results demonstrated that ROCK1-siRNA treatment alleviated IRI-induced hepatocellular apoptosis/necrosis in Nrf2$^{M\text{-}KO}$ mice (Figure 8F). Moreover, markedly reduced macrophage and neutrophil infiltration was detected in the IR stress-induced livers of ROCK1-siRNA–treated Nrf2$^{M\text{-}KO}$ mice (Figure 8G-I). As shown in Figure 8J, ROCK1-siRNA treatment inhibited the mRNA levels of TNF-α, IL-6, MCP-1, and iNOS but increased IL-10 levels in the IR stress-induced livers of Nrf2$^{M\text{-}KO}$ mice. Moreover, ROCK1-siRNA treatment significantly reduced IR-induced ROS and MDA production and increased GSH activity in the ischemic livers of Nrf2$^{M\text{-}KO}$ mice (Figure 8K).

DISCUSSION

This study documents the regulatory role of macrophage Nrf2 in innate immune responses through Timp3-mediated RhoA/ROCK pathway activation in inflammatory responses and liver injury during liver IRI. The principal findings are as follows: (i) macrophage Nrf2 expression is increased and negatively correlates with IR stress-induced liver injury in clinical patients who underwent OLT or hepatectomy; (ii) macrophage Nrf2 deficiency as established by the *Cre-LoxP* system increases liver ROS, inflammation, and injury during liver IR; (iii) Nrf2 deficiency inhibits the target gene Timp3, which is required for the activation of the RhoA/ROCK pathway; and (iv) the RhoA/ROCK pathway is crucial for Nrf2 deficiency-mediated worsening of IR stress-induced liver ROS, inflammation, and injury. Our results highlight the importance of the macrophage Nrf2-Timp3 axis as a key regulator of RhoA/ROCK pathway-mediated innate immune responses during liver IR (Figure 8L).

Nrf2 is a transcription factor associated with various intracellular signaling pathways that protect organs against oxidative stress and the inflammatory response.[15-17] Under normal conditions, Nrf2 is retained in the cytoplasm by binding to Keap1, which promotes the ubiquitination/proteolysis of Nrf2.[30,31] Various endogenous or exogenous stimuli dissociate Nrf2 from Keap1, which leads to the nuclear translocation of Nrf2 and the activation of cytoprotective target genes, thus protecting cells from excessive ROS damage and inflammatory responses. Indeed, Nrf2 regulates genes that are involved in two major redox systems: the GSH and thioredoxin systems.[32,33] In addition to redox homeostasis, Nrf2 is an important regulator of inflammation and has also been examined in numerous models of asthma, emphysema, and sepsis.[34-36] Additionally, the link between innate immune responses and the Nrf2 pathway may serve as a bridge between immune responses and ROS through the regulation of inflammation. Nrf2-deficient mice are likely to exhibit exacerbated inflammation during the overproduction of ROS.[36]

Several studies have shown that the depletion of Nrf2 increases susceptibility to toxin-induced liver injury, all of which effectively indicate that the Nrf2 pathway is protective.[15-17] In addition, Nrf2 activation attenuates liver IRI in mice. Specifically, the effect of hepatocyte-specific Nrf2 induction was investigated, and activation of the Nrf2-ARE pathway in hepatocytes decreased hepatocellular damage, apoptosis, inflammation, and ROS during liver IRI.[24] Accumulating evidence has suggested that hepatic macrophages are critical for the liver immune response against IR.[1,2,26-29] Activation of liver macrophages directly results in the release of several inflammatory mediators, which contribute directly and indirectly to hepatocyte death/apoptosis. Moreover, the release of intracellular constituents from stressed/necrotic cells due to any cause (including hypoxia, stress, and chemicals) promotes hepatic macrophage activation.[7,8,37,38] In liver IRI, the liberation of danger

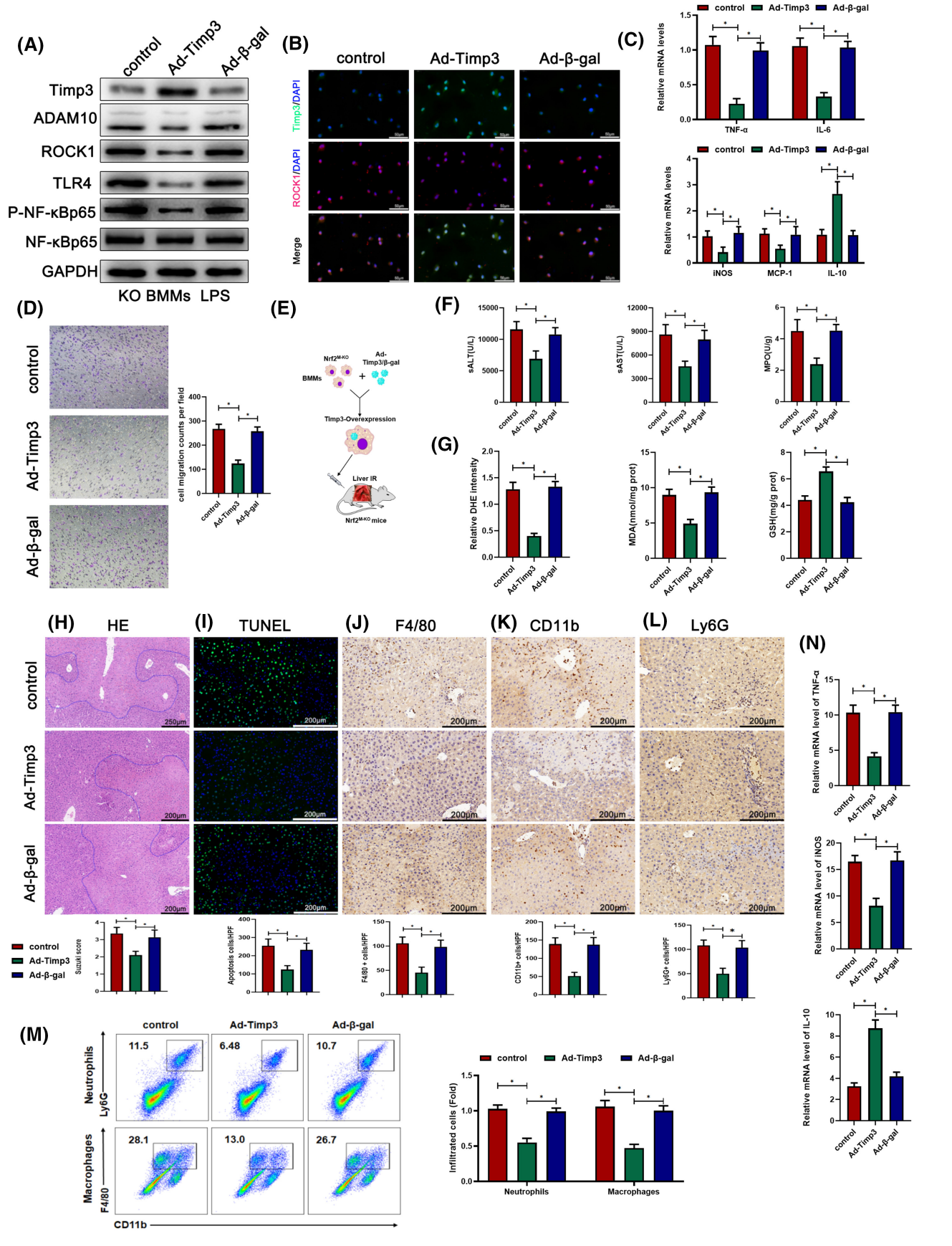
(A)
control
Ad-Timp3
Ad-β-gal
Timp3
ADAM10
ROCK1
TLR4
P-NF-κBp65
NF-κBp65
GAPDH
KO BMMs LPS
(B)
control
Ad-Timp3
Ad-β-gal
Timp3/DAPI
ROCK1/DAPI
Merge
(C)
control
Ad-Timp3
Ad-β-gal
Relative mRNA levels
TNF-α
IL-6
iNOS
MCP-1
IL-10
(D)
control
Ad-Timp3
Ad-β-gal
cell migration counts per field
(E)
Nrf2M-KO BMMs
Ad-Timp3/β-gal
Timp3-Overexpression
Liver IR
Nrf2M-KO mice
(F)
sALT(U/L)
sAST(U/L)
MPO(U/g)
(G)
Relative DHE intensity
MDA(nmol/mg prot)
GSH(mg/g prot)
(H)
HE
(I)
TUNEL
(J)
F4/80
(K)
CD11b
(L)
Ly6G
250μm
200μm
Suzuki score
Apoptosis cells/HPF
F4/80 + cells/HPF
CD11b+ cells/HPF
Ly6G+ cells/HPF
(N)
Relative mRNA level of TNF-α
Relative mRNA level of iNOS
Relative mRNA level of IL-10
(M)
control
Ad-Timp3
Ad-β-gal
11.5
6.48
10.7
28.1
13.0
26.7
Neutrophils
Ly6G
Macrophages
F4/80
CD11b
Infiltrated cells (Fold)
Neutrophils
Macrophages

FIGURE 6 Ad-Timp3 BMMs prevents IR-induced hepatocellular damage in Nrf2$^{M\text{-}KO}$ mice. The IR model mice were subjected to 90 min of partial liver warm ischemia, followed by 6 h of reperfusion. BMMs, from Nrf2$^{M\text{-}KO}$ mice, were transfection with Ad-Timp3 or Ad-β-gal. Nrf2$^{M\text{-}KO}$ mice were performed IRI model after infusion of Ad-Timp3 Nrf2$^{M\text{-}KO}$ BMMs, Ad-β-gal Nrf2$^{M\text{-}KO}$ BMMs, or untreated Nrf2$^{M\text{-}KO}$ BMMs as control respectively. (A) These transfected BMMs were incubated with LPS (100 ng/mL) for 6 h. Timp3, ADAM10, ROCK1, TLR4, P-NF-κBp65, and NF-κBp65 protein expression levels measured by WB. (B) Dual immunofluorescence staining of Timp3 (green), ROCK1 (red), and DAPI (blue) in these transfected BMMs. (C) Detection of TNF-α, IL-6, MCP-1, iNOS, and IL-10 by qRT-PCR in these BMMs cultured with LPS (100 ng/mL, 3 h). (D) Transwell assay analyzed the migratory ability of BMMs with LPS for 24 h. (E) sALT and sAST levels were measured. (F) MPO activities of ischemic livers. (G) Quantitation of ROS-sensing dye DHE staining, MDA, and GSH activities were assessed in ischemic liver tissues. (H-L) HE staining, TUNEL staining, F4/80 TUNEL staining, CD11b staining, and Ly6G staining. (M) Flow cytometry analysis was conducted to examine the accumulation of neutrophils and macrophages in livers from mice subjected to 6 h postreperfusion in each group. (N) Detection of TNF-α, iNOS, and IL-10 by qRT-PCR in ischemic livers. $n = 6$, $^*p < 0.05$ by Student t test

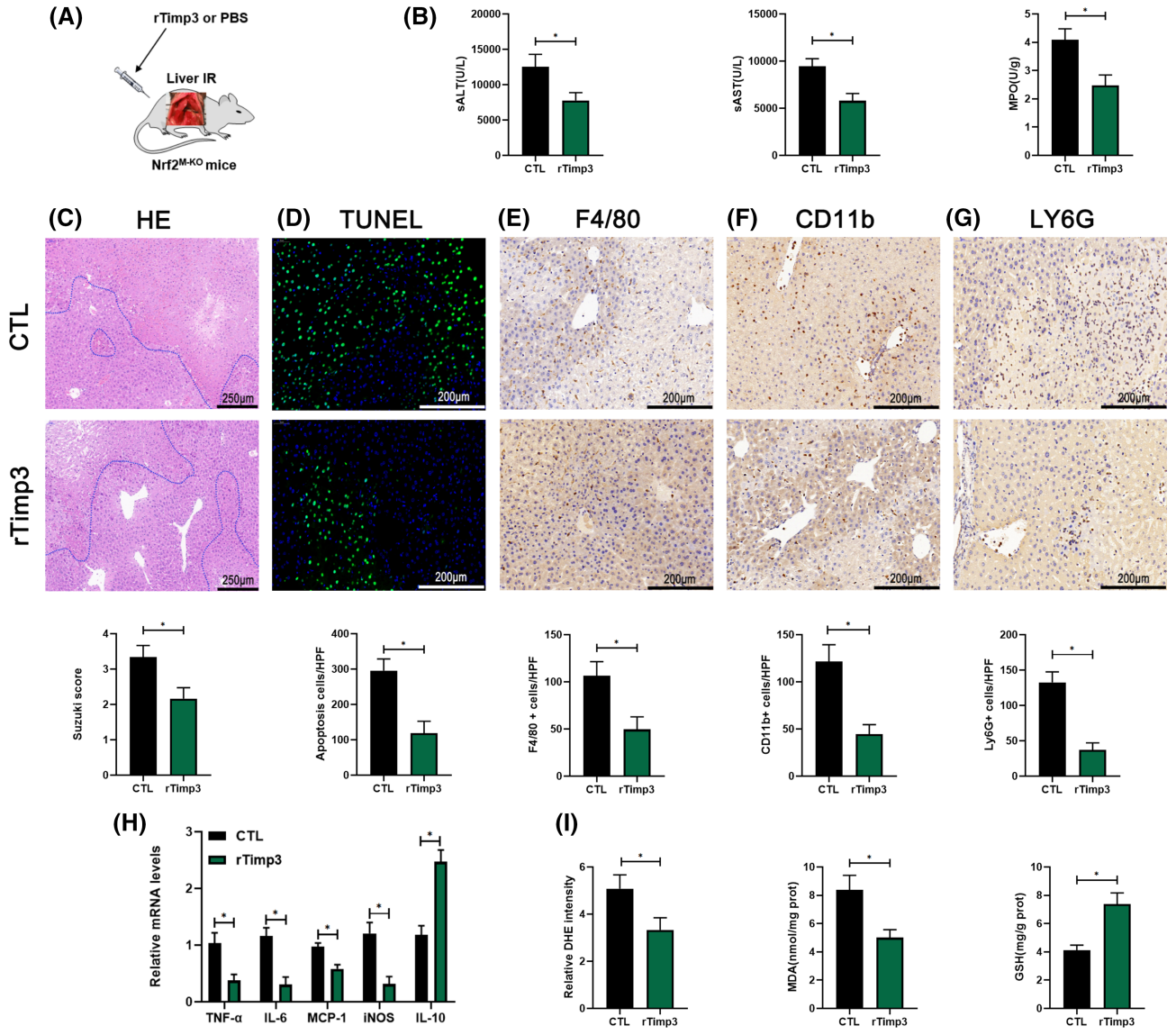

FIGURE 7 rTimp3 prevents IR-induced hepatocellular damage in Nrf2$^{M\text{-}KO}$ mice. The IR model mice were subjected to 90 min of partial liver warm ischemia, followed by 6 h of reperfusion. (A) Nrf2M-KO mice were treated with rTimp3 (100 ng/kg) 1 h before establishing hepatic IRI model. (B) sALT and sAST levels were measured. MPO activities of ischemic livers. (C-G) HE staining, TUNEL staining, F4/80 staining, CD11b staining, and Ly6G staining. (H) Detection of TNF-α, IL-6, MCP-1, iNOS, and IL-10 by qRT-PCR in ischemic livers. (I) Quantitation of ROS-sensing dye DHE staining, MDA, and GSH activities were assessed in ischemic liver tissues. $n = 6$, $^*p < 0.05$ by Student t test

signals from inflamed, necrotic, or hypoxic parenchymal cells directly contributes to macrophage activation. Furthermore, our previous studies showed that ATF3 attenuates liver injury by activating Nrf2/HO-1 signaling to protect against TLR4-driven inflammation in macrophages after IRI.[23] To further analyze the

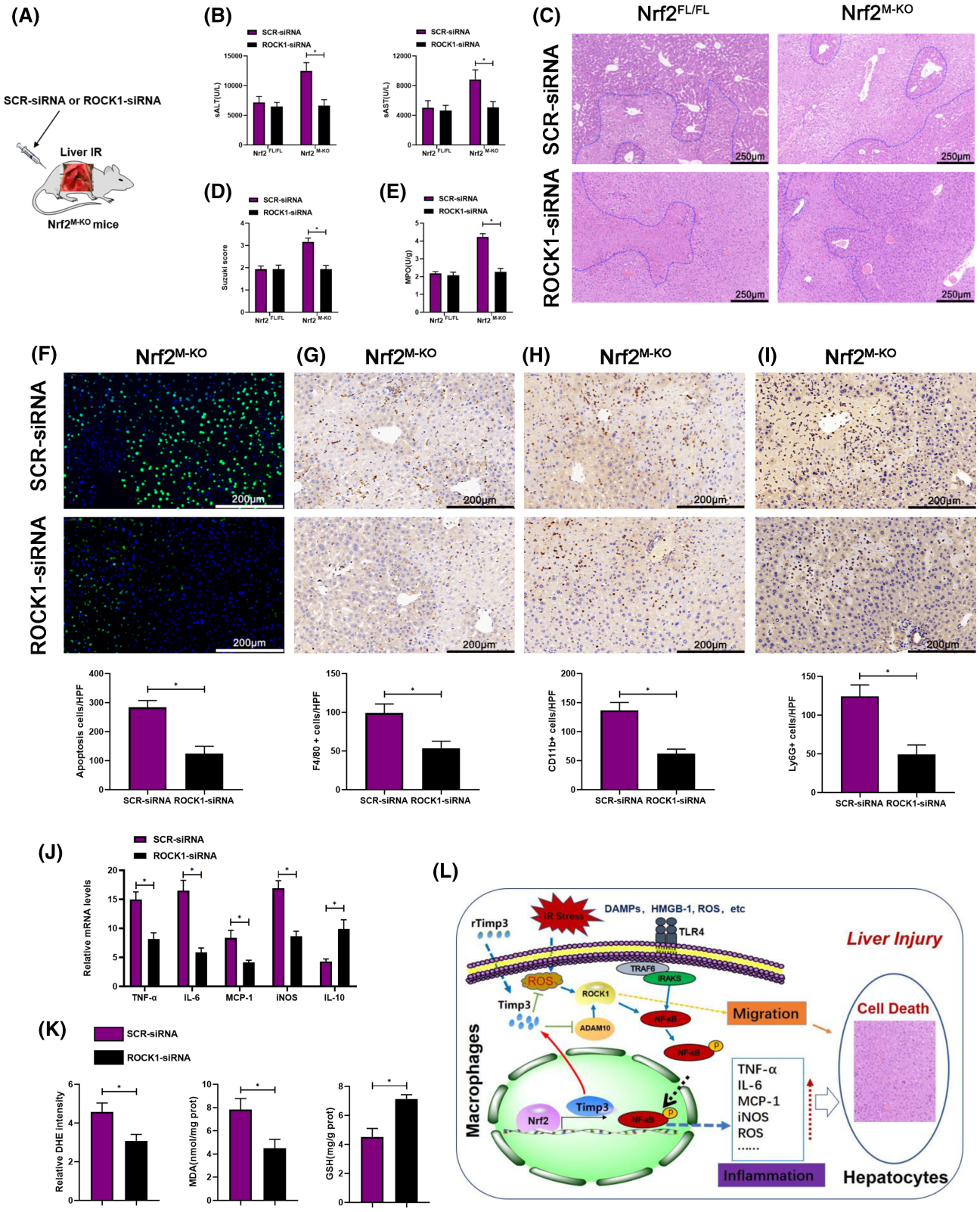

FIGURE 8 Inhibition of ROCK pathway rescue Nrf2$^{M\text{-}KO}$-related inflammation and injury in ischemic livers. The IR model mice were subjected to 90 min of partial liver warm ischemia, followed by 6 h of reperfusion. (A) Some Nrf2FL/FL and Nrf2M-KO mice were injected through tail vein with ROCK1-siRNA or SCR-siRNA (2 mg/kg). (B) sALT and sAST levels were measured. (C,D) Representative HE staining of ischemic liver tissues; scale is 250 μm; liver damage was evaluated by Suzuki's histological score. (E) MPO activities of ischemic livers. (F-I) TUNEL staining, F4/80 staining, CD11b staining, and Ly6G staining. (J) Detection of TNF-α, IL-6, MCP-1, iNOS, and IL-10 by qRT-PCR in ischemic livers. (K) Quantitation of ROS-sensing dye DHE staining, MDA, and GSH activities were assessed in ischemic liver tissues. (L) Schematic illustration how macrophage Nrf2 may regulate Timp3-mediated RhoA/ROCK pathway in innate immune activation during liver IRI. $n = 6$, $^*p < 0.05$ by Student t test

roles of macrophage Nrf2, we assessed the degree of injury to ischemic livers by the Cre-LoxP system to create a myeloid-specific Nrf2-deficient strain. As expected, macrophage Nrf2 deficiency significantly increased liver IRI, as evidenced by increased levels of serum transaminase, damaged hepatic architecture, and the promotion of hepatocellular necrosis/apoptosis. Moreover, macrophage Nrf2 deletion increased ROS production, elevated proinflammatory cytokines, and boosted CD68+ macrophage/Ly6G+ neutrophil infiltration. Thus, our data suggest that macrophage-specific Nrf2 attenuates liver inflammation and injury through the inhibition of innate immune activation during IR.

One striking finding was that Timp3 expression was significantly inhibited in Nrf2-deficient macrophages. Timp3 belongs to the family of Timps, which includes four members. Timps play a vital role in inhibiting matrix metalloproteinases (MMPs), disintegrin and metalloproteinases (ADAMs), and ADAM with thrombospondin motifs (ADAMTSs), which are involved in the formation of extracellular matrix.[39] Timp3 is different from other members (Timp1, 2, and 4) in many ways; for example, Timp3 is characterized by poor aqueous solubility and a high affinity for proteoglycans and has the broadest range of substrates, including all MMPs and multiple ADAMs and ADAMTSs.[40] Numerous studies have revealed the important role of Timp3 in various pathophysiological conditions and diseases, including nonalcoholic steatohepatitis, HCC, liver fibrosis, IRI, interstitial nephritis, and fibrosis.[41-45] Herein, we found that Nrf2 binds to the promoter of Timp3 and increases the expression of Timp3 in macrophages. Importantly, Ad-Timp3 or rTimp3 reduced ROS production and TLR4-mediated innate inflammation and rescued IR stress-induced liver injury in macrophage-specific Nrf2-deficient mice. Consistent with our results, Timp3 upregulation reduces cardiac IRI by inhibiting myocardial apoptosis through the inhibition of the ROS pathway.[46]

It is reported that Timp knockout increases ADAM10 expression and secretion by exosomes in fibroblasts.[47] Consistently, we found that Nrf2 deficiency led to low expression of Timp3, which also enhanced ADAM10 expression in macrophages. ADAM10 effectively activates the RhoA/ROCK pathway in some conditions.[47] Indeed, ROS also causes activation of the RhoA/ROCK pathway.[48,49] Thus, Timp3 may play a critical role in the Nrf2-regulated RhoA/ROCK pathway in macrophages in the presence of ROS. Interestingly, our result is opposite to that of a previous report showing that NRF2 increases the RhoA/ROCK pathway in breast cancer.[25] The different regulatory roles of NRF2 may be different and dependent on the animal models under different physiological or pathological conditions, which should be further investigated. Some evidence suggests that RhoA/ROCK may act as a "molecular switch" in the activation of TLR4-mediated innate immune responses. Activation of the RhoA/ROCK pathway promotes monocyte/leukocyte accumulation in the context of tissue injury. Specific inhibition of the ROCK pathway prevents NF-κB activation and the inflammatory response in different inflammatory diseases.[50,51] Activation of Rho/Rho kinase signaling in hepatic stellate cells is associated with increased susceptibility to IRI in steatotic livers.[52] Our previous studies demonstrated that activation of the RhoA/ROCK pathway triggers the innate immune response and increases IR-induced inflammatory injury in myeloid-specific Notch1-deficient livers.[53] Thus, RhoA/ROCK activation may be critical for promoting $Nrf2^{M\text{-}KO}$-mediated IR-induced liver inflammation and injury. Notably, the expression of ADAM10 and ROCK1 was significantly increased in Nrf2-deficient macrophages in vivo and in vitro. Moreover, suppression of the macrophage ROCK pathway effectively rescued $Nrf2^{M\text{-}KO}$-related liver inflammation and injury during liver IRI.

In conclusion, our findings demonstrate that macrophage-specific Nrf2 deficiency promotes the RhoA/ROCK signaling pathway and exacerbates liver damage by repressing the target gene Timp3 in IR stress-induced livers. By identifying the molecular pathways by which the macrophage Nrf2-Timp3 axis regulates RhoA/ROCK-mediated innate immunity, our findings provide a rationale for therapeutic approaches to ameliorate sterile inflammatory liver injury.

ACKNOWLEDGEMENTS

We are grateful to Dr. Siddhartha Biswas (Greater Kailash Hospital, India) for his constructive criticism on the manuscript and revising the English text.

CONFLICT OF INTEREST

The authors disclose no conflicts of interest.

AUTHOR CONTRIBUTIONS

Jianhua Rao, Jiannan Qiu, Ming Ni, and Ling Lu were involved in study design, conducted the experiments, and drafted the paper; Jiannan Qiu, Ming Ni, Feng Cheng, Hao Wang, Peng Wang, Lei Zhang, Zeng Wang, and Mu Liu performed the experiments; Jiannan Qiu, Ming Ni, Feng Cheng, Jianhua Rao, and Ling Lu provided material support; Feng Cheng, Ming Ni, Xuehao Wang, and Ling Lu commented the manuscript; and Jianhua Rao, Feng Cheng, Xuehao Wang, and Ling Lu supervised the study and wrote the paper.

REFERENCES

1. Zhai Y, Petrowsky H, Hong JC, Busuttil RW, Kupiec-Weglinski JW. Ischemia-reperfusion injury in liver transplantation–from bench to bedside. Nat Rev Gastroenterol Hepatol. 2013;10(2):79–89.
2. Zhou H, Wang H, Ni M, Yue S, Xia Y, Busuttil RW, et al. Glycogen synthase kinase 3β promotes liver innate immune activation by restraining AMP-activated protein kinase activation. J Hepatol. 2018;69(1):99–109.

3. Panel M, Ruiz I, Brillet R, Lafdil F, Teixeira-Clerc F, Nguyen CT, et al. Small-molecule inhibitors of cyclophilins block opening of the mitochondrial permeability transition pore and protect mice from hepatic ischemia/reperfusion injury. Gastroenterology. 2019;157(5):1368–82.
4. Schwabe RF, Brenner DA. Mechanisms of liver injury. I. TNF-alpha-induced liver injury: role of IKK, JNK, and ROS pathways. Am J Physiol Gastrointest Liver Physiol. 2006;290(4):G583–9.
5. Kamo N, Ke B, Ghaffari AA, Shen XD, Busuttil RW, Cheng G, et al. ASC/caspase-1/IL-1β signaling triggers inflammatory responses by promoting HMGB1 induction in liver ischemia/reperfusion injury. Hepatology. 2013;58(1):351–62.
6. Rao J, Cheng F, Zhou H, Yang W, Qiu J, Yang C, et al. Nogo-B is a key mediator of hepatic ischemia and reperfusion injury. Redox Biol. 2020;37:101745.
7. Hennig P, Garstkiewicz M, Grossi S, Di Filippo M, French LE, Beer HD. The crosstalk between Nrf2 and inflammasomes. Int J Mol Sci. 2018;19(2):562.
8. Katsuoka F, Yamamoto M. Small Maf proteins (MafF, MafG, MafK): History, structure, and function. Gene. 2016;586(2):197–205.
9. McMahon M, Thomas N, Itoh K, Yamamoto M, Hayes JD. Redox-regulated turnover of Nrf2 is determined by at least two separate protein domains, the redox-sensitive Neh2 degron, and the redox-insensitive Neh6 degron. J Biol Chem. 2004;279(30):31556–67.
10. Silva-Islas CA, Maldonado PD. Canonical and non-canonical mechanisms of Nrf2 activation. Pharmacol Res. 2018;134:92–9.
11. Suzuki T, Yamamoto M. Stress-sensing mechanisms and the physiological roles of the Keap1-Nrf2 system during cellular stress. J Biol Chem. 2017;292(41):16817–24.
12. Liu M, Grigoryev DN, Crow MT, Haas M, Yamamoto M, Reddy SP, et al. Transcription factor Nrf2 is protective during ischemic and nephrotoxic acute kidney injury in mice. Kidney Int. 2009;76(3):277–85.
13. Warpsinski G, Smith MJ, Srivastava S, Keeley TP, Siow RCM, Fraser PA, et al. Nrf2-regulated redox signaling in brain endothelial cells adapted to physiological oxygen levels: Consequences for sulforaphane mediated protection against hypoxia-reoxygenation. Redox Biol. 2020;37:101708.
14. Ashrafian H, Czibik G, Bellahcene M, Aksentijević D, Smith A, Mitchell S, et al. Fumarate is cardioprotective via activation of the Nrf2 antioxidant pathway. Cell Metab. 2012;15(3):361–71.
15. Parada E, Buendia I, León R, Negredo P, Romero A, Cuadrado A, et al. Neuroprotective effect of melatonin against ischemia is partially mediated by alpha-7 nicotinic receptor modulation and HO-1 overexpression. J Pineal Res. 2014;56(2):204–12.
16. Wei Y, Gong J, Yoshida T, Eberhart CG, Xu Z, Kombairaju P, et al. Nrf2 has a protective role against neuronal and capillary degeneration in retinal ischemia-reperfusion injury. Free Radic Biol Med. 2011;51(1):216–24.
17. Calvert JW, Jha S, Gundewar S, Elrod JW, Ramachandran A, Pattillo CB, et al. Hydrogen sulfide mediates cardioprotection through Nrf2 signaling. Circ Res. 2009;105(4):365–74.
18. Sun Q, Meng QT, Jiang Y, Xia ZY. Ginsenoside Rb1 attenuates intestinal ischemia reperfusion induced renal injury by activating Nrf2/ARE pathway. Molecules. 2012;17(6):7195–205.
19. Ke B, Shen XD, Zhang YU, Ji H, Gao F, Yue S, et al. KEAP1-NRF2 complex in ischemia-induced hepatocellular damage of mouse liver transplants. J Hepatol. 2013;59(6):1200–7.
20. Yi Z, Deng M, Scott MJ, Fu G, Loughran PA, Lei Z, et al. Immune-responsive gene 1/itaconate activates nuclear factor erythroid 2-related factor 2 in hepatocytes to protect against liver ischemia-reperfusion injury. Hepatology. 2020;72(4):1394–411.
21. Rao J, Qian X, Li G, Pan X, Zhang C, Zhang F, et al. ATF3-mediated NRF2/HO-1 signaling regulates TLR4 innate immune responses in mouse liver ischemia/reperfusion injury. Am J Transplant. 2015;15(1):76–87.
22. Lv Z, Xu X, Sun Z, Yang YX, Guo HU, Li J, et al. TRPV1 alleviates osteoarthritis by inhibiting M1 macrophage polarization via Ca2+/CaMKII/Nrf2 signaling pathway. Cell Death Dis. 2021;12(6):504.
23. Wall SB, Li R, Butler B, Burg AR, Tse HM, Larson-Casey JL, et al. Auranofin-mediated NRF2 induction attenuates interleukin 1 beta expression in alveolar macrophages. Antioxidants (Basel). 2021;10(5):632.
24. Ko E, Kim D, Min DW, Kwon SH, Lee JY. Nrf2 regulates cell motility through RhoA-ROCK1 signalling in non-small-cell lung cancer cells. Sci Rep. 2021;11(1):1247.
25. Zhang C, Wang H-J, Bao Q-C, Wang L, Guo T-K, Chen W-L, et al. NRF2 promotes breast cancer cell proliferation and metastasis by increasing RhoA/ROCK pathway signal transduction. Oncotarget. 2016;7(45):73593–606.
26. Ke B, Shen XD, Gao F, Ji H, Qiao BO, Zhai Y, et al. Adoptive transfer of ex vivo HO-1 modified bone marrow-derived macrophages prevents liver ischemia and reperfusion injury. Mol Ther. 2010;18(5):1019–25.
27. Yue S, Zhu J, Zhang M, Li C, Zhou X, Zhou M, et al. The myeloid heat shock transcription factor 1/β-catenin axis regulates NLR family, pyrin domain-containing 3 inflammasome activation in mouse liver ischemia/reperfusion injury. Hepatology. 2016;64(5):1683–98.
28. Tang ZY, Loss G, Carmody I, Cohen AJ. TIMP-3 ameliorates hepatic ischemia/reperfusion injury through inhibition of tumor necrosis factor-alpha-converting enzyme activity in rats. Transplantation. 2006;82(11):1518–23.
29. Rao J, Yue S, Fu Y, Zhu J, Wang X, Busuttil RW, et al. ATF6 mediates a pro-inflammatory synergy between ER stress and TLR activation in the pathogenesis of liver ischemia-reperfusion injury. Am J Transplant. 2014;14(7):1552–61.
30. McMahon M, Itoh K, Yamamoto M, Hayes JD. Keap1-dependent proteasomal degradation of transcription factor Nrf2 contributes to the negative regulation of antioxidant response element-driven gene expression. J Biol Chem. 2003;278(24):21592–600.
31. Cullinan SB, Gordan JD, Jin J, Harper JW, Diehl JA. The Keap1-BTB protein is an adaptor that bridges Nrf2 to a Cul3-based E3 ligase: oxidative stress sensing by a Cul3-Keap1 ligase. Mol Cell Biol. 2004;24(19):8477–86.
32. Corsello T, Komaravelli N, Casola A. Role of Hydrogen Sulfide in NRF2- and Sirtuin-Dependent Maintenance of Cellular Redox Balance. Antioxidants (Basel). 2018;7(10):129.
33. Jones DP. Radical-free biology of oxidative stress. Am J Physiol Cell Physiol. 2008;295(4):C849–68.
34. Rangasamy T, Guo J, Mitzner WA, Roman J, Singh A, Fryer AD, et al. Disruption of Nrf2 enhances susceptibility to severe airway inflammation and asthma in mice. J Exp Med. 2005;202(1):47–59.
35. Ishii Y, Itoh K, Morishima Y, Kimura T, Kiwamoto T, Iizuka T, et al. Transcription factor Nrf2 plays a pivotal role in protection against elastase-induced pulmonary inflammation and emphysema. J Immunol. 2005;175(10):6968–75.
36. Thimmulappa RK, Lee H, Rangasamy T, Reddy SP, Yamamoto M, Kensler TW, et al. Nrf2 is a critical regulator of the innate immune response and survival during experimental sepsis. J Clin Invest. 2006;116(4):984–95.
37. Mossanen JC, Krenkel O, Ergen C, Govaere O, Liepelt A, Puengel T, et al. Chemokine (C-C motif) receptor 2-positive monocytes aggravate the early phase of acetaminophen-induced acute liver injury. Hepatology. 2016;64(5):1667–82.
38. Starkey Lewis P, Campana L, Aleksieva N, Cartwright JA, Mackinnon A, O'Duibhir E, et al. Alternatively activated macrophages promote resolution of necrosis following acute liver injury. J Hepatol. 2020;73(2):349–60.
39. Takawale A, Sakamuri SS, Kassiri Z. Extracellular matrix communication and turnover in cardiac physiology and pathology. Compr Physiol. 2015;5(2):687–719.

40. Fan D, Kassiri Z. Biology of tissue inhibitor of metalloproteinase 3 (TIMP3), and its therapeutic implications in cardiovascular pathology. Front Physiol. 2020;11:661.
41. Jiang JX, Chen X, Fukada H, Serizawa N, Devaraj S, Török NJ. Advanced glycation endproducts induce fibrogenic activity in nonalcoholic steatohepatitis by modulating TNF-α-converting enzyme activity in mice. Hepatology. 2013;58(4):1339–48.
42. Defamie V, Sanchez O, Murthy A, Khokha R. TIMP3 controls cell fate to confer hepatocellular carcinoma resistance. Oncogene. 2015;34(31):4098–108.
43. Azar F, Courtet K, Dekky B, Bonnier D, Dameron O, Colige A, et al. Integration of miRNA-regulatory networks in hepatic stellate cells identifies TIMP3 as a key factor in chronic liver disease. Liver Int. 2020;40(8):2021–33.
44. Fujii T, Duarte S, Lee E, Ke B, Busuttil RW, Coito AJ. Tissue inhibitor of metalloproteinase 3 deficiency disrupts the hepatocyte E-cadherin/β-catenin complex and induces cell death in liver ischemia/reperfusion injury. Liver Transpl. 2020;26(1):113–26.
45. Kassiri Z, Oudit GY, Kandalam V, Awad A, Wang X, Ziou X, et al. Loss of TIMP3 enhances interstitial nephritis and fibrosis. J Am Soc Nephrol. 2009;20(6):1223–35.
46. Liu H, Jing X, Dong A, Bai B, Wang H. Overexpression of TIMP3 protects against cardiac ischemia/reperfusion injury by inhibiting myocardial apoptosis through ROS/Mapks pathway. Cell Physiol Biochem. 2017;44(3):1011–23.
47. Shimoda M, Principe S, Jackson HW, Luga V, Fang H, Molyneux SD, et al. Loss of the Timp gene family is sufficient for the acquisition of the CAF-like cell state. Nat Cell Biol. 2014;16(9):889–901.
48. Montezano AC, Callera GE, Yogi A, He Y, Tostes RC, He G, et al. Aldosterone and angiotensin II synergistically stimulate migration in vascular smooth muscle cells through c-Src-regulated redox-sensitive RhoA pathways. Arterioscler Thromb Vasc Biol. 2008;28(8):1511–8.
49. Kondrikov D, Caldwell RB, Dong Z, Su Y. Reactive oxygen species-dependent RhoA activation mediates collagen synthesis in hyperoxic lung fibrosis. Free Radic Biol Med. 2011;50(11):1689–98.
50. Segain JP, Raingeard de la Blétière D, Sauzeau V, Bourreille A, Hilaret G, Cario-Toumaniantz C, et al. Rho kinase blockade prevents inflammation via nuclear factor kappa B inhibition: evidence in Crohn's disease and experimental colitis. Gastroenterology. 2003;124(5):1180-7.
51. Mong PY, Wang Q. Activation of Rho kinase isoforms in lung endothelial cells during inflammation. J Immunol. 2009;182(4):2385–94.
52. Kuroda S, Tashiro H, Igarashi Y, Tanimoto Y, Nambu J, Oshita A, et al. Rho inhibitor prevents ischemia-reperfusion injury in rat steatotic liver. J Hepatol. 2012;56(1):146–52.
53. Lu L, Yue S, Jiang L, Li C, Zhu Q, Ke M, et al. Myeloid Notch1 deficiency activates the RhoA/ROCK pathway and aggravates hepatocellular damage in mouse ischemic livers. Hepatology. 2018;67(3):1041–55.

SUPPORTING INFORMATION

Additional supporting information may be found in the online version of the article at the publisher's website.

How to cite this article: Rao J, Qiu J, Ni M, Wang H, Wang P, Zhang L, et al. Macrophage nuclear factor erythroid 2-related factor 2 deficiency promotes innate immune activation by tissue inhibitor of metalloproteinase 3–mediated RhoA/ROCK pathway in the ischemic liver. Hepatology. 2022;75:1429–1445. https://doi.org/10.1002/hep.32184